

# 70 years of lake evolution and glacial lake outburst floods in the Cordillera Blanca (Peru) and implications for the future

Adam Emmer<sup>a,\*</sup>, Stephan Harrison<sup>b</sup>, Martin Mergili<sup>c,d</sup>, Simon Allen<sup>e</sup>, Holger Frey<sup>e</sup>, Christian Huggel<sup>e</sup>

<sup>a</sup> The Czech Academy of Sciences, Global Change Research Institute, Brno, Czechia

<sup>b</sup> College of Life and Environmental Sciences, Exeter University, Exeter, UK

<sup>c</sup> Institute of Applied Geology, University of Natural Resources and Life Sciences (BOKU), Vienna, Austria

<sup>d</sup> Department of Geography and Regional Research, University of Vienna, Vienna, Austria

<sup>e</sup> Department of Geography, University of Zürich, Zürich, Switzerland

## ARTICLE INFO

### Article history:

Received 21 January 2020

Received in revised form 21 March 2020

Accepted 21 March 2020

Available online 25 April 2020

### Keywords:

Andes

Climate forcing

GLOFs

GLOF response time

Lag time

Peak frequency

Post-Little Ice Age

Topographic control

## ABSTRACT

Climate change, glacier retreat and glacial lake outburst floods (GLOFs) are intertwined. The Cordillera Blanca in Peru has one of the world's longest GLOF records and here we assess the evolution of glacial lakes in the region between 1948 and 2017 and investigate the links to documented GLOFs. We also model future lake evolution under two climate scenarios to provide an assessment of current and future GLOF triggering potential. Our analysis shows that the number of lakes as well as the total lake area has increased during the historical period. The formation of new lakes is, however, not uniform among different lake types with bedrock-dammed lakes exhibiting the largest increase in recent decades. We argue that moraine-dammed lakes have already formed at the majority of potential locations in the Cordillera Blanca and that the next generation of lakes which are expected to form in response to glacier retreat over topographically suitable areas will be predominantly bedrock-dammed. Based on a regional GLOF inventory, we show that the peak frequency of GLOFs occurred from the late 1930s to early 1950s. While GLOFs originating from moraine-dammed lakes dominated in this period, recent GLOFs have originated from bedrock-dammed lakes. At the same time, the majority of GLOFs originated from lakes in a proglacial phase (i.e. in contact with glacier), even though the share of proglacial lakes did not exceed 12% at any time step during the analysed period. While many moraine-dammed lakes evolved into the glacier-detached evolutionary phase, bedrock-dammed lakes became a major lake dam type among proglacial lakes. Over the remainder of the 21st century, a further increase in lake area of up to 10% is anticipated, with up to 50 new bedrock dammed lakes likely to develop as glaciers retreat. There is little difference in lake development and GLOF triggering potential under climate scenarios driven by RCP 2.6 and 8.5. Based on topographic disposition, recent and future lakes do not individually appear more or less susceptible to landslide impact than lakes that already developed earlier in the 20th century. Synthesizing these findings, we forecast that bedrock-dammed lakes will become the dominant source of GLOFs in the next decades. Because such dams are inherently more stable, we expect overall lower GLOF magnitudes compared to documented GLOFs from moraine-dammed lakes.

© 2020 Elsevier B.V. All rights reserved.

## 1. Introduction

### 1.1. Climate change and the occurrence of GLOFs

The global climate change-induced glacier recession affecting the majority of high mountains since the end of the Little Ice Age (LIA) is associated with the formation and evolution of glacial lakes, and accompanied by concerns about changing hazards of glacial lake outburst floods (GLOFs). These form sudden releases of water from glacial lakes with potentially harmful consequences for nature and societies (Clague

et al., 2012; Huss et al., 2017; Harrison et al., 2018; Vuille et al., 2018). As a result, there is increasing scientific and policy interest in better understanding the nature and timing of such impacts. Despite increasing scientific and policy interest in GLOFs (see the overview of Emmer, 2018), very little is known about the regional drivers of the timing of GLOF occurrence. While numerous studies focus on developing lake inventories (e.g. Petrov et al., 2017; Wilson et al., 2018) or analysing glacial lake outburst floods (e.g. Veh et al., 2019) in specific regions, these are usually limited to the relatively short period of available satellite data (mostly Landsat). This restricts comprehensive insights into the evolution of lakes and outburst floods in the broader post-LIA context.

Recent progress in increasing the availability and completeness of regional GLOF inventories and databases (e.g. Carrivick and Tweed,

\* Corresponding author.

E-mail addresses: [emmer.a@czechglobe.cz](mailto:emmer.a@czechglobe.cz), [aemmer@seznam.cz](mailto:aemmer@seznam.cz) (A. Emmer).

2016) allowed Harrison et al. (2018) to show regionally lagged responses to the end of the LIA leading to a global increase in GLOF frequency in the 1930s. It was shown that different regions worldwide are expected to have different lag times to post-LIA climate change; firstly, due to the regional differences in the timing of the end of the LIA (e.g. Mann et al., 2008; Ahmed et al., 2013) and, secondly, due to the different dynamics of glacier response to the post-LIA climate change (Harrison et al., 2018). These recent research findings suggest that lake formation and GLOF occurrence should be rather homogeneous within a certain geographic region, but asynchronous globally.

### 1.2. Study area: the Cordillera Blanca

Our study area – the Cordillera Blanca in Peru ( $8.5^{\circ}$ – $10.0^{\circ}$  S;  $77^{\circ}$ – $78^{\circ}$  W; see Fig. 1) – is the most heavily glacierized tropical mountain range (with 25% of the world's tropical glaciers; Kaser and Osmaston, 2002) and a prominent area for GLOF research and risk management, with research going back to the 1940s (Carey, 2005; Carey et al., 2012; Emmer et al., 2018). The area of interest is defined by the border of the Huascarán National Park (HNP), covering 3600 km<sup>2</sup>. The main part of the Cordillera Blanca is formed by granodiorite and tonalite rocks (CB batholith; IGM, 1975), uplifted during the Cenozoic Era (Coldwell et al., 2011), while the outer parts are mainly formed by sedimentary and metamorphic rocks (IGM, 1975). All the peaks of the Cordillera Blanca towering above 6000 m asl are located within the HNP, including Huascarán (6768 m asl) – the highest mountain in Peru. Cenozoic uplift, climate variability and associated geomorphological processes resulted in dissected mountain relief with a wide variety of glacial, glacialfluvial and periglacial landforms. Glaciers of the Cordillera Blanca have been

largely receding since the end of the LIA (Rabatel et al., 2013; Schauwecker et al., 2014), which is dated in this region to 1880 (Thompson et al., 2000; Solomina et al., 2007). This has resulted in the formation and evolution of lakes (Iturrizaga, 2014; Emmer et al., 2016) and in a high concentration of lake outburst floods, some of which have been disastrous (Liboutry et al., 1977; Zapata, 2002; Carey, 2005; Emmer, 2017).

### 1.3. Aims of this study

Using the example of the Cordillera Blanca, the main aims of this study are: (i) to provide detailed insights into the evolution of lakes during the period 1948–2017; (ii) to elucidate the topographic controls of this evolution; (iii) to link findings with recent models of GLOF development since the end of the post-LIA (i.e. Harrison et al., 2018); and (iv) to assess future scenarios of GLOF patterns. Synthesizing these parts, we aim to introduce a general and transferable schematic model of GLOF formation in time, considering different lake dam types and phases of lake evolution.

## 2. Data and methods

### 2.1. Lake inventories 1948–2017

Remotely sensed images covering the period 1948–2017 were used for the analysis of region-wide lake evolution in time as well as the evolution of individual lakes. These include three sets of aerial images (1948–1950, 1962 and 1970; AI), Landsat images available at the USGS LandsatLook Viewer (1975–2018; LL) and high-resolution images

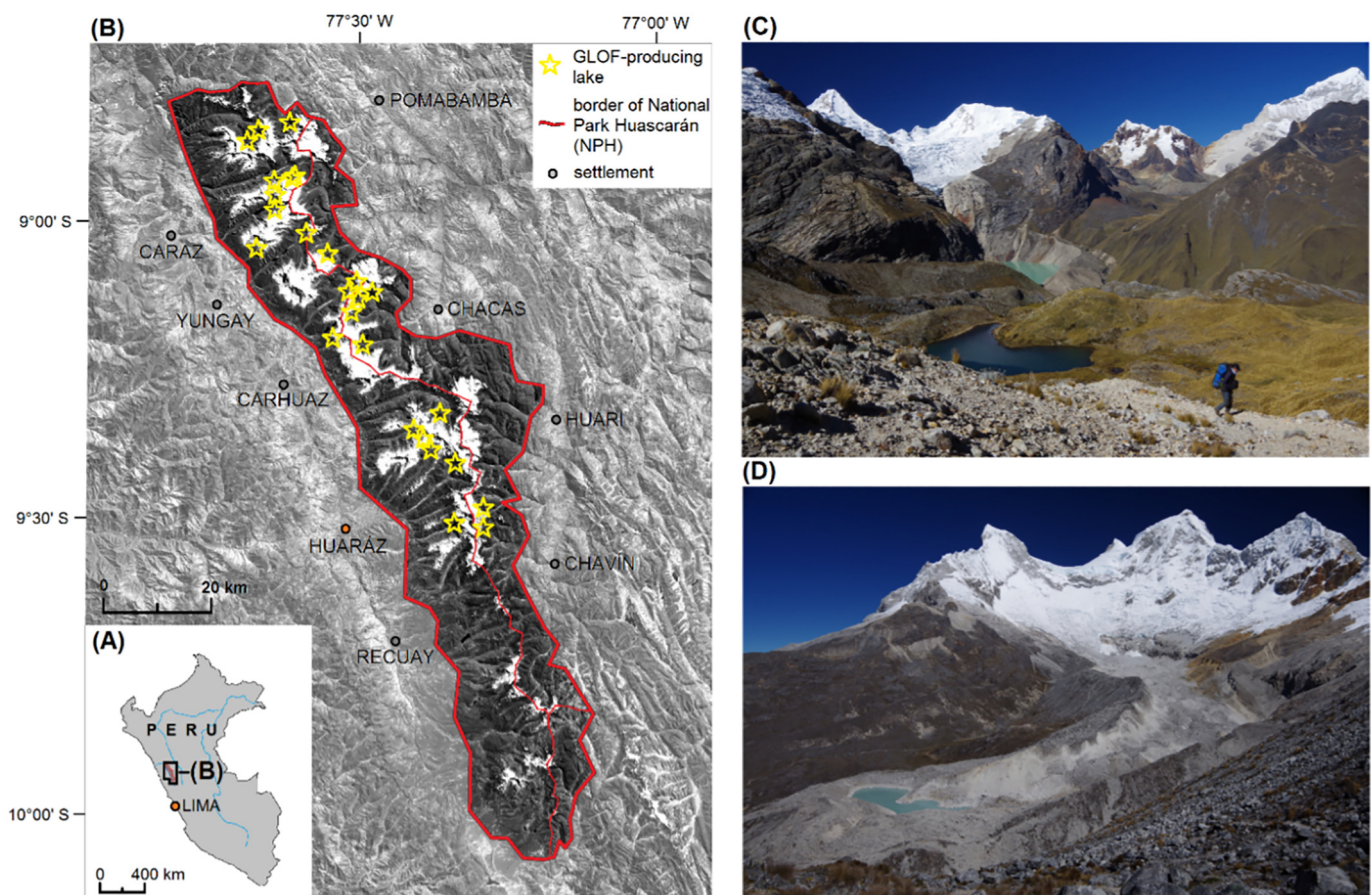


**Fig. 1.** Study area Cordillera Blanca. (A) shows the location of the study area in Peru; (B) displays a satellite image (Landsat) with the highlighted area of the Huascarán National Park; GLOF-producing lakes analysed in this study are indicated; (C) illustrates the dissected mountainous relief in the Alpamayo Valley, Northern Cordillera Blanca; the GLOF-producing lake Jancurish is visible in the centre of the image; (D) shows the Southeast face of the Huandoy massif (6395 m asl) with a recently formed lake visible in the frontal part of the glacier.



of various origins available at Google Earth Digital Globe PRO (2003–2018; GE). No usable images are available for the 1980s. Seven lake inventories have been produced (see Table S1) by visual interpretation of optical remotely sensed images for the following time steps: 1948–1950 (AI); 1962 (AI); 1970 (AI); 1991 (LL), 2001–2003 (LL, GE), 2010–2011 (GE) and 2017–2018 (GE). The reference 2017–2018 inventory is an updated version of the [Emmer et al. \(2016\)](#) lake inventory.

Each lake in each time step is described by two qualitative characteristics - the lake dam type and the phase of the evolution. Five different lake dam types are distinguished in this study: (i) moraine-dammed; (ii) bedrock-dammed; (iii) combined dams (typically bedrock with thin moraine cover); (iv) ice-dammed (supraglacial lakes); and (v) not specified. Landslide-dammed lakes are only considered in the analyses of the total lake area. Five different phases of evolution are distinguished: (i) future lake site (i.e. the site where lakes form after the analysed period 1948–2017); (ii) (a group of) supraglacial ponds; (iii) proglacial lake; (iv) glacier-detached lake; and (v) no lake (failed, dried out). Examples of the most common lake dam types and different evolution phases are shown in [Fig. 2](#). The Mann-Kendall trend test ([Aziz et al., 2003](#)) has been used to explore the trends in time series, e.g. the trend in the number and share of different lake dam types and phases of evolution.

Some of the datasets are not complete or the quality of the images did not allow visual interpretation, especially for earlier lake inventories and some of the Landsat images. These missing data represent up to 8.4% of the total number of lakes in 1948. Potential errors caused by these missing data in the estimation of total number and area of lakes are indicated by error bars. To estimate this error, we sum the areas of these lakes derived from the next step in time where lake areas were available, assuming that the maximum size of the lakes in the dataset with missing data is not larger than in the subsequent dataset. Half of this sum is then added to the total area of visible lakes and used as the size of the potential error. This error is <2% of the total lake area for the 1948 dataset and <1% for all other time steps. The potential error induced by manual drawing of lake polygons is not quantified in this study.

## 2.2. The analysis of topographic control

For the first-order analyses of topographic control on lake formation, we postulate that the presence of rather flat areas generally indicates a favorable environment for the formation of lakes ([Frey et al., 2010](#)).

Analysing these patterns at a very general scale only, we accept the limitations that (i) lakes do not necessarily form in flat areas, but mainly in depressions; (ii) glacier surfaces do not necessarily serve as a surrogate for the corresponding rock surface; and (iii) existing lakes are included and may bias the statistics derived. We only consider those trends visible with both the 5° and the 10° slope threshold. The hypsometric distribution of flat areas between 3500 m and 5500 m, here defined as areas with a local slope of  $\leq 5^\circ$  and  $\leq 10^\circ$  within a 50 m elevation range, respectively, derived from an SRTM V4 DEM resampled to  $90 \times 90$  m cell size is analysed. A5 and A10 represent the absolute areas, p5 and p10 the percent of the total area A in the corresponding elevation range. Glacier extent data were derived from [Hidrandina \(1970\)](#), [Georges \(2004\)](#), [INAIGEM \(2016\)](#), and [Veettil \(2018\)](#).

## 2.3. GLOF inventory

Large amounts of documented data exist for the study area of the Cordillera Blanca, providing detailed insights on disastrous events going back to the 18th century ([Zapata, 2002](#)). Using these data (reports, old maps, geotechnical drawings and field photos from the archive of the Autoridad Nacional del Agua, Huaráz, Peru) and verifying them with remotely sensed images (1948–2016) and field surveys, a comprehensive inventory of 28 GLOFs from moraine-dammed lakes has been presented by [Emmer \(2017\)](#), including both dam failures (18 cases) and dam overtoppings (10 cases). In addition, 4 GLOFs from bedrock-dammed lakes are considered in this study (data from [Liboutry et al., 1977](#); [Carey et al., 2012](#); [Emmer et al., 2016](#)). Three classes of GLOF magnitude are distinguished, according to the reach of the flood ([Emmer, 2017](#)): (i) minor (reach <2 km; overall slope of the trajectory  $10\text{--}25^\circ$ ); (ii) major (reach 2–10 km; overall slope of the trajectory  $<10^\circ$ ); and (iii) extreme (reach >10 km; overall slope of the trajectory  $<8^\circ$ ). In terms of reported GLOFs, the Cordillera Blanca region is among the best-documented regions worldwide and as such provides a unique opportunity to study the frequency of GLOF occurrence for a time period going back to the 1st half of the 20th century.

## 2.4. Future lake evolution

The erosive power of glaciers can form large depressions at the bed and when such overdeepened parts are exposed due to glacier retreat

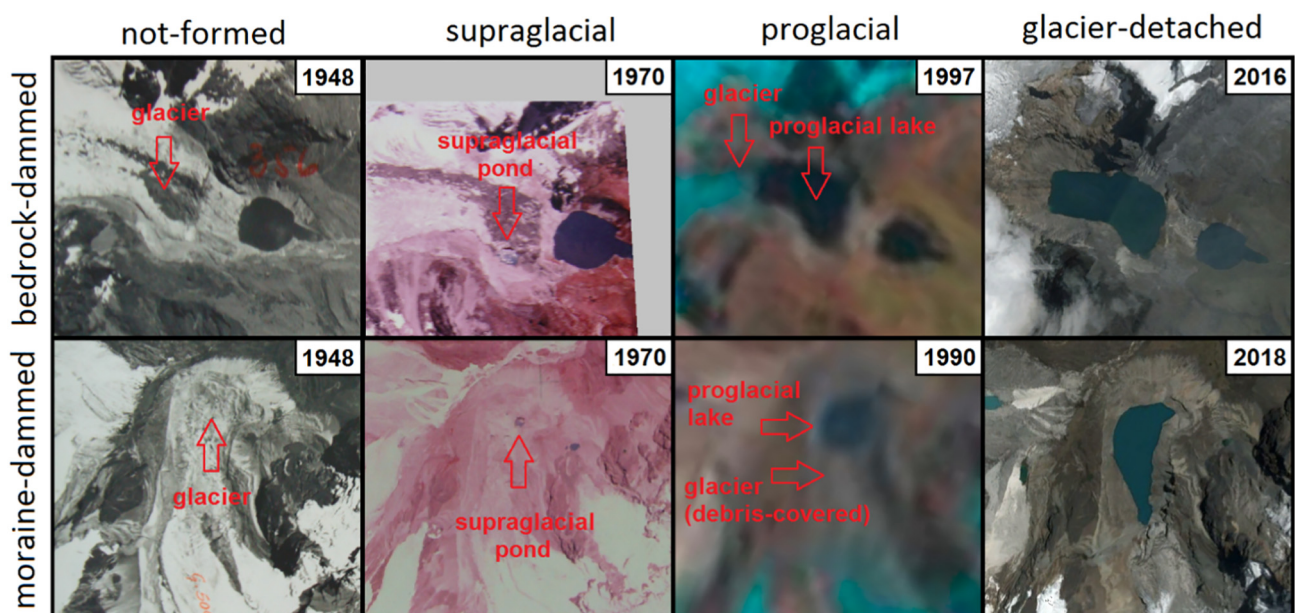


**Fig. 2.** Different phases of lake evolution with examples of bedrock-dammed Lake Maparaju ( $9^\circ 28' 18''$  S,  $77^\circ 18' 30''$  W; 4628 m asl) and moraine-dammed Lake Quitacocha ( $8^\circ 52' 49''$  S,  $77^\circ 41' 06''$  W; 4755 m asl). Images: archive of the Autoridad Nacional del Agua (Huaráz, Peru), Landsat (USGS LandsatLook) and CNES/Airbus (Google Earth Digital Globe).

and filled with water, rather than sediments, new lakes can form (Evans and Clague, 1994). By detecting overdeepenings in the glacier bed, sites of potential future lake formation and possible expansion of existing lakes can therefore be identified. For this purpose, the GIS-based model GlabTop was developed for estimating ice-thickness distribution and bed topography across the Swiss Alps (Linsbauer et al., 2012; Paul and Linsbauer, 2012). The modelled ice thickness distribution is subtracted from a surface DEM to obtain the bed topography, i.e., a DEM without glaciers, from which overdeepenings in the glacier bed can be detected and analysed. The current study uses the results from Colonia et al. (2017), who applied GlabTop across the Peruvian Andes, identifying potential overdeepenings larger than 0.01 km<sup>2</sup>. To determine how many of these overdeepenings will be uncovered to potentially develop into lakes by the end of the 21st century, modelled glacial extents for the Cordillera Blanca under RCPs 2.6 and 8.5 were taken from Schauwecker et al. (2017), who assessed the glacier area under future scenarios based on a relationship with the freezing level height. To calculate the total lake area at the end of the 21st century, the mapped lake extent in 2018 (considering only lakes >0.01 km<sup>2</sup>) is combined with the modelled overdeepenings exposed under RCPs 2.6 and 8.5 respectively.

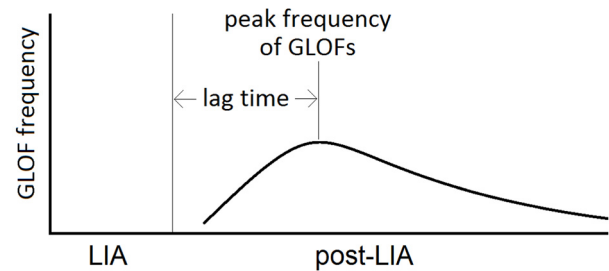
### 2.5. GLOF triggering potential

We consider the potential for GLOF triggering based on the likelihood for ice and/or rock avalanches to strike a lake, a known main triggering process of GLOFs, and the only possible mechanism by which an outburst can occur from a bedrock dammed lake. The assessment procedure is based on the concept of topographic potential (Romstad et al., 2009) which encompasses (a) the potential for rock or ice to detach (parameterised by slope angle) and (b) the potential for the resulting rock and/or ice avalanche to reach a glacial lake (parameterised by the overall trajectory slope or angle of reach). This concept has been integrated within a comprehensive GLOF risk assessment for the Swiss Alps (Schaub, 2015), and for Northwest India (Allen et al., 2016) and Tibet (Allen et al., 2019). We do not distinguish between whether the slope is bedrock, ice-covered, or debris, and assume that an impact into a lake is possible from any slope >30° (Allen et al., 2011; Fischer et al., 2012) where the overall slope trajectory is >14° ( $\tan \alpha = 0.25$ ) (Romstad et al., 2009; Noetzi et al., 2003). Within each lake watershed, the  $\tan \alpha$  values for all grid cells fulfilling these two criteria were summed, to give a quantitative measure of the potential for avalanches to trigger an outburst from that lake. In this way, steep slopes located closer to a lake (i.e., from which an ice and/or rock avalanche is more likely to reach the lake), automatically contribute more to the overall triggering potential. For the historical lake inventories and future scenarios, we use the ASTER GDEM at 30 m resolution. Testing showed that the choice of using the current or future (ice-free) DEM has very little influence on the results, as the bed topography closely approximates the current surface topography.

### 2.6. Estimating LRT, GRT and lag time

A conceptual model of the occurrence of GLOFs was first introduced by Clague and Evans (2000), suggesting moraine construction during cooler and/or wetter periods (when glaciers advance) and lake formation during warmer and/or drier periods (when glaciers retreat). GLOF frequency generally increases until reaching the peak (peak frequency of GLOF occurrence) in this model, which may be decades after glaciers have started to retreat. This time period between the beginning of warming and the peak frequency of GLOF occurrence is termed the *lag time*. After reaching the peak, the following decades are characterized by a generally decreasing frequency of GLOFs in this model (see Fig. 3A). From the perspective of individual lakes, the *lag time* is the period between the beginning of glacier recession and a GLOF from this lake. As such, the lag time of individual GLOF-producing lakes has two components: (i) limnological response time (LRT; i.e. the period

### (A) region



### (B) lake

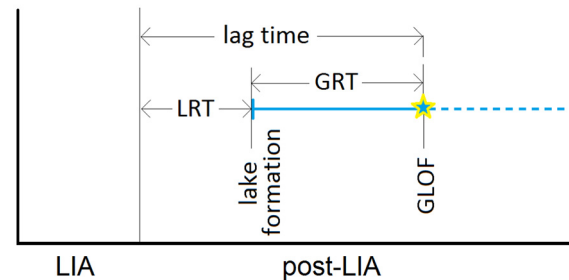


**Fig. 3.** Graphical representation of lag time of GLOF peak frequency within a region (A) and limnological response time (LRT), GLOF response time (GRT) and lag time of an individual lake (B). Dashed line in (B) indicates that lake may persist or not after the GLOF. Part (A) is modified from Clague and Evans (2000).

between the beginning of warming (i.e. the end of the LIA) and the formation of a lake (appearance)); and (ii) GLOF response time (GRT; i.e. the period of time between lake formation (appearance) and a GLOF event occurring); hence *lag time* = LRT + GRT (Harrison et al., 2018; see Fig. 3B). While the termination of the LIA is dated to 1880s in the Cordillera Blanca (Thompson et al., 2000; Solomina et al., 2007), lake formation is derived from aerial images (the first appearance; most commonly in supraglacial or proglacial stage) and/or documentary data, where available (see above).

## 3. The evolution of lakes

The evolution of lakes in the Cordillera Blanca is analysed for the period 1948–2017, considering different lake dam types, phases of evolution as well as total lake area change (see Fig. 4). Five different lake dam types and four phases of evolution are distinguished in this study (see Fig. 2; see also Data and methods).

The overall number of lakes gradually increased from  $643 \pm 32$  lakes in 1948 to 893 lakes in 2017 and the total lake area increased from  $27.98 \pm 0.48$  km<sup>2</sup> in 1948 to 35.22 km<sup>2</sup> in 2018 (see Fig. 4A, B and Table S1; the 1948 error is induced by missing data for some parts of the study area; see Data and methods). This increase has a rather linear character. An increasing trend in the number of lakes of all different lake dam types is confirmed using a Mann-Kendall trend test (confidence factors (CF) > 99.0%; see Table S2) with the exception of not specified lakes (no trend; CF = 76.4%). The share of individual lake dam types (see Fig. 4C), however, shows certain differences among them.

The share of moraine-dammed lakes and lakes with combined dams (bedrock dam with moraine cover) remained stable over time (CF = 88.1%), ranging from 37.9% in 1970 to 34.8% in 2010 for moraine-dammed lakes and from 17.6% in 1970 to 15.6% in 2017 for lakes with combined dams. In contrast, bedrock-dammed lakes and ice-dammed lakes show an increasing trend (CF = 98.5% and 96.5%, respectively), ranging from 25.4% in 1970 to 32.3% in 2017 for bedrock-dammed lakes and from 1.7% in 1990 to 3.5% in 2017 for ice-dammed lakes. The share of not specified lakes displays a decreasing trend (CF = 100.0%).

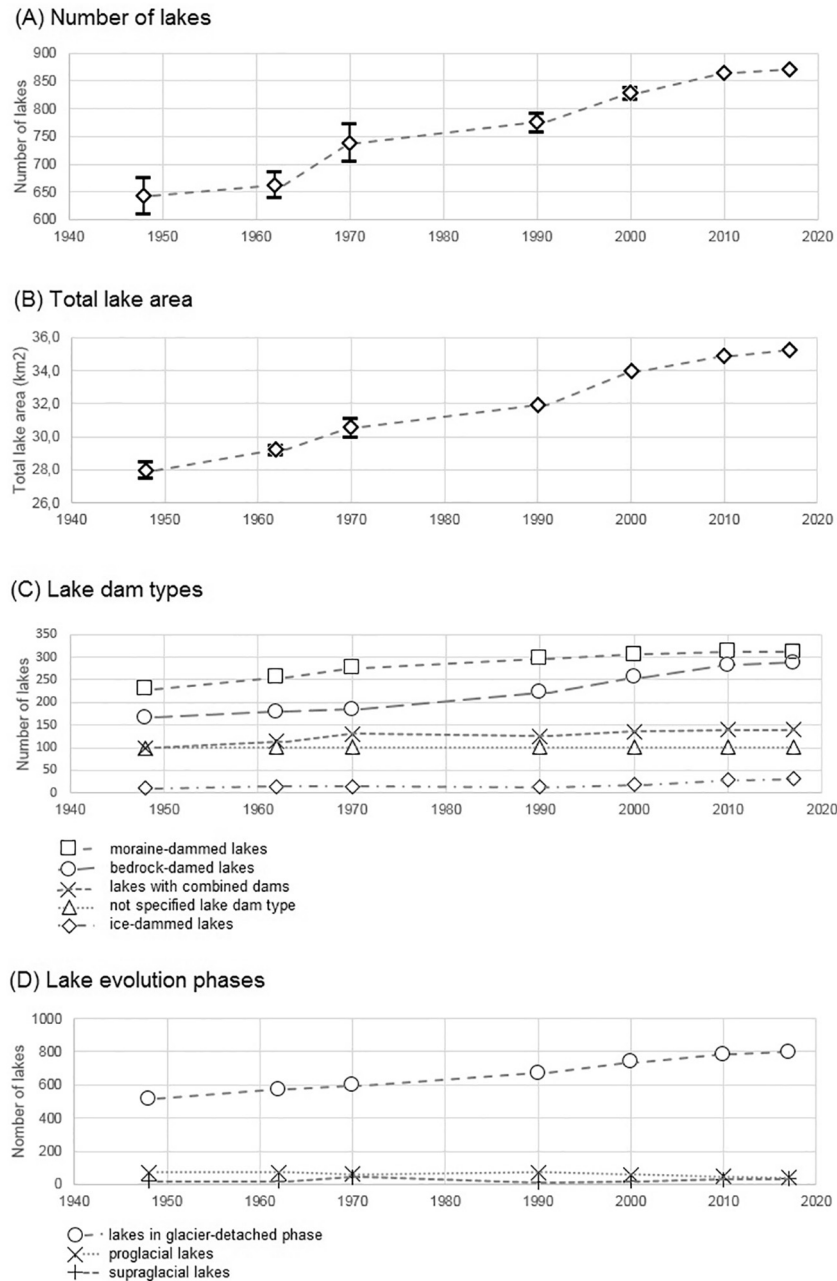


**Fig. 4.** The evolution of lakes in the Cordillera Blanca between 1948 and 2017. (A) shows the total number of lakes; (B) shows the total lake area; (C) shows the share of different lake dam types; and (D) shows the share of different phases of evolution. Potential errors induced by missing data are indicated for (A) and (B).

In terms of different phases of lake evolution (see Fig. 4D), we show that the number as well as the share of lakes in the glacier-detached phase (lakes detached from glacier termini) displays an increasing trend (CF = 100.0%). While there were 517 glacier-detached lakes in 1948 (i.e. 85.2% of all lakes in 1948), this number increased to 798 in 2017 (91.7% of all). In contrast, the number as well as the share of lakes in the proglacial phase displays a decreasing trend (CF = 96.5% and 99.9% respectively). While 71 proglacial lakes are observed in 1948 (11.7% of all lakes in 1948), 74 are observed in 1990 (9.7% of all) and 40 in 2017 (4.6% of all). The number of supraglacial lakes shows no trend (CF = 66.7%) while the share of supraglacial lakes remains stable over time, however with CF = 50.0%. A shift is observed for different evolution phases and individual lake dam types (see Fig. 2). While 56 out of 71 proglacial lakes (i.e. 78.9% of all) were moraine-dammed in 1948, 30 out of 40 proglacial lakes (i.e. 75.0%) were bedrock-dammed in 2017 (see Table S1).

#### 4. Topographic control on lake formation

We analysed the topography of the Cordillera Blanca, assuming that lakes are expected to form preferentially in generally flat terrain defined as A5 and A10 (total area with slope  $\leq 5^\circ$  and  $\leq 10^\circ$ ), respectively p5 and p10 (i.e. per cent of the total area with the slope  $\leq 5^\circ$  and  $\leq 10^\circ$ ). A general decreasing trend is detected in p5 and p10 between 3500 m and 5150 m asl (see Fig. 5). Above 4500 m, the total area (A) drops steadily with elevation, making the trend of A5 and A10 even stronger. Below 4500 m, there is a peak in A5, A10, p5, and p10 at 4200 m, most likely representing biases introduced by particular areas such as Lake Parón, including flat upstream areas. A slight peak is also visible between 4500 m and 4600 m, indicating a number of lakes or former lake basins associated with terminal moraines from the LIA (e.g. Lake Palcacocha, Lake Milluacocha). The notable peak in p5 and p10 (to a lesser extent in A5 and A10 due to the low values of A) between 5150 m and



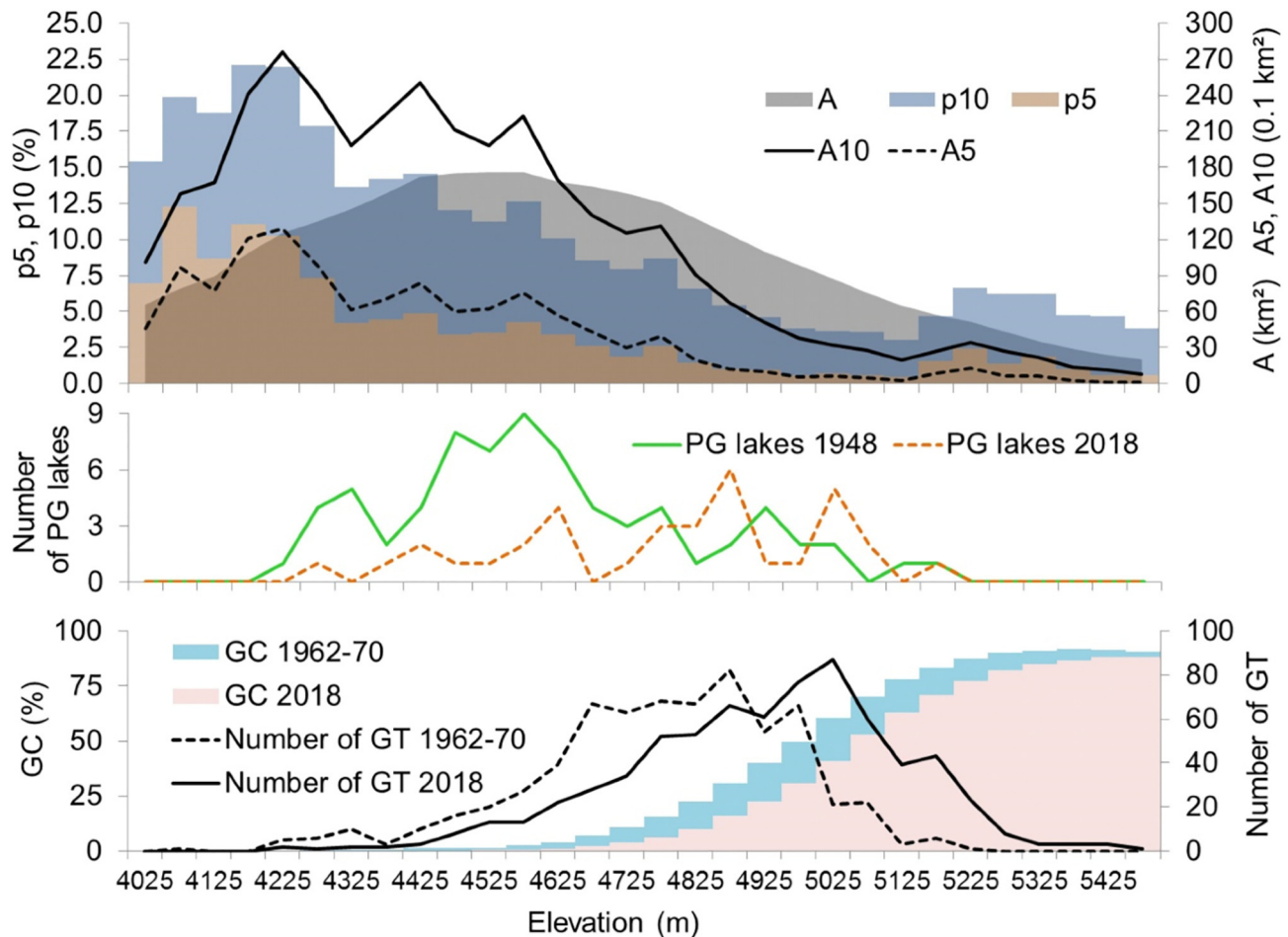


**Fig. 5.** Topographic setting of the Cordillera Blanca. Top: Areas favorable for lake formation (flat areas A5 and A10, p5 and p10) in different elevational classes are shown. Middle: The elevational distribution of proglacial lakes (PG) shows a shift to higher levels from 1948 to 2018. Bottom: Glacier coverage (GC) and number of glacier termini (GT) per elevation.

5450 m represents the area above the steep troughs of the glacial valleys, but still below the cirques and walls of the highest peaks of the Cordillera Blanca.

In summary, we observe a clear decrease of areas potentially suitable for lake development from 4600 m to 5150 m, which is the elevation range over which glaciers were retreating between the LIA and the early 21st century. This pattern may explain the slightly decreasing proportion of proglacial lakes in the analysed period. The concentration of lakes around 4600 m asl is explained by the abundance of LIA terminal moraines which form dams. However, Fig. 5 also shows that further glacial retreat could again expose a larger surface area suitable for the formation of lakes, which are likely to be dammed by bedrock (Colonía et al., 2017). The increased appearance of bedrock-dammed lakes at higher elevation, which is already observed now (see Fig. S1), could be an early indicator of such a trend (see also Section 5.4).

## 5. GLOFS, their causes and the lag time concept

### 5.1. Documented GLOFs and phases of lake evolution

A total of 32 GLOFs are documented from the Cordillera Blanca, 28 of which originated from moraine-dammed lakes (1725–2003; see Emmer, 2017) and 4 from bedrock-dammed lakes (1970–2012; Lliboutry et al., 1977; Carey et al., 2012; Emmer et al., 2016). Considering only those GLOFs with a known year of occurrence ( $n = 26$ ), the evident peak frequency of GLOFs from moraine-dammed lakes is observed between the late 1930s and the early 1950s, using different moving average windows (see Fig. S2). Extreme and major GLOFs are concentrated in

this period. The lag time of this peak is, thus, 60–80 years since the end of the LIA, dated to the 1880s (Thompson et al., 2000; Solomina et al., 2007). A clearly distinguishable secondary peak is observed in 1970, when 5 GLOFs occurred, all of them, however, as a result of the catastrophic earthquake on 31st May 1970. A third peak of GLOFs from moraine-dammed lakes is observed between 1997 and 2003 when 4 events occurred. The most recent GLOFs originated from bedrock-dammed lakes.

To understand the frequencies of GLOFs and their relation to climate variability and change as well as glacier recession, individual lakes and their evolution need to be examined. Table S3 shows the evolution of 28 lakes which produced GLOFs since the end of the LIA. Four of these lakes do not exist anymore and four of the lakes produced two GLOFs. Twenty GLOF-producing lakes (71.4%) changed their phase of evolution during the analysed period 1948–2018. At least 17 out of 32 analysed GLOFs (53.1%) occurred from lakes in the proglacial phase of their evolution, suggesting an increased occurrence of GLOFs during this evolutionary phase, especially considering the comparably low share of proglacial lakes in all time steps, decreasing from 11.7% in 1948 to 4.6% in 2017 (see Fig. 4B). At least 10 GLOFs (31.2%) occurred from lakes in the glacier-detached phase of their evolution, whereas the phase of evolution of 5 lakes at the time of GLOF occurrence is not known.

### 5.2. Regional causes of GLOFs

Specific causes and mechanisms of GLOFs are known or can be estimated in 21 cases (65.6%). A majority of these ( $n = 15$ ; 71.4%) are thought to be caused by different types of landslides into lakes

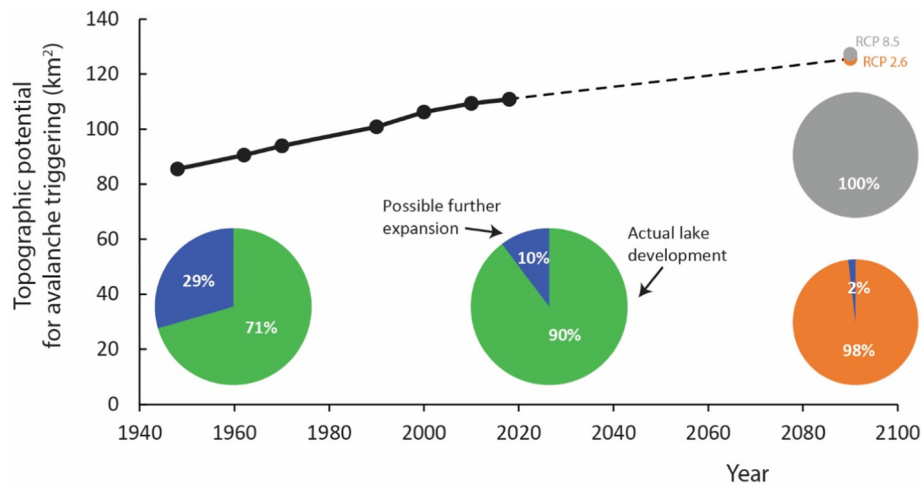


**Fig. 6.** Topographic potential for landslides of ice and/or rock to trigger an outburst event, based on historical mapped lake outlines, and modelled future lake extents under RCP 2.6 and 8.5. Topographic potential considers the area above each lake where slopes are steep enough and close enough to the lake to threaten it. The pie charts compare the actual stage of lake development in 1948, 2018, and at the end of the 21st century, with the maximum possible lake area.

(e.g., ice avalanches, rock avalanches, landslides from the moraines surrounding lakes; not including earthquake-induced landslides). Extreme and major GLOFs in the peak frequency period from the late 1930s to the 1950s were frequently caused by calving processes/ice avalanches (e.g., Lake Artesoncocha, Lake Jancarurish; see also [Emmer, 2017](#)), which might be linked to the El Niño phase of ENSO at that time.

The El Niño phase of ENSO is accompanied by heavy rain in Peru, especially in the north, and associated with the intrusion of warm tropical waters along the coast that allows deep convection in a region where cold upwelling waters and semi-arid to arid climatic conditions usually prevail ([Rein et al., 2005](#); [Bourrel et al., 2015](#)). However, detailed hydrometeorological and climatological data to assess the impact of El Niño events on mountain processes in Peru are sparse. While climatological and hydrological observational data for Peru are available (e.g. PISCO, Peruvian-interpolated data from the National Service of Meteorology and Hydrology of Peru) these only date back to 1981 ([Sulca et al., 2018](#)). In addition, the influence of the high-mountain topography on climate and weather processes introduces considerable uncertainties in successfully interpolating data between instrumental sites ([MauSSION et al., 2014](#); [Rau et al., 2017](#)).

Three GLOFs occurred during the 1997–1998 El Niño event. Two of these are documented to have been caused by landslides from lateral moraines into the lake. The occurrence of slope movements in moraines might be caused by heavy precipitation ([Klimeš et al., 2016](#)) and these GLOFs, therefore, might be attributed to El Niño forcing, which usually brings extreme rainfall events to the Cordillera Blanca. However, despite the fact that some general links were identified between the phases of ENSO and landslides reported in the Ancash region ([Vilímek et al., 2014](#)), direct evidence allowing us to link El Niño and the occurrence of GLOFs is still missing.

Apart from possibly climate-driven GLOFs, five events are attributed to the disastrous 1970 Ancash earthquake on 31st May. This peak of GLOF occurrence is stochastic in time and magnitude and may influence the statistics of post-LIA GLOFs without any causal link to the stages of glacier retreat and phases of lake evolution. This leads us to the conclusion that long-term climate, glacier and lake evolution sets region-wide preconditions for GLOFs (e.g., an increased share of lakes in the GLOF-susceptible proglacial phase), whereas specific events trigger them, highlighting the need for complex (considering wide range of possible triggers) and multi-scale (both region-wide and individual lake-targeting) monitoring and assessment. Moreover, several peak frequencies of GLOFs might be observed in high mountainous terrain with multiple generations of topographic overdeepenings associated with previous glacial activity.

### 5.3. The lag time concept, limnological response time (LRT) and GLOF response time (GRT)

We show that the LRT varies considerably among individual GLOF-producing lakes (see Table S3). Considering different dam types of GLOF-producing lakes, we show that the duration of LRTs is typically <70 years for GLOF-producing moraine-dammed lakes and >80 years for GLOF-producing bedrock-dammed lakes in the Cordillera Blanca; GRTs typically vary between 5 and 30 years and there are no differences among different lake dam types. In some specific cases, GRT may be considerably longer (e.g. Lake Librón which may have existed before the LIA). Examples of GRT in order of  $10^3$  years were reported from the Patagonian Andes ([Pánek et al., 2018](#)). Further, our dataset shows four examples of lakes which produced GLOFs following the period of the most rapid glacier retreat and lake growth. However, similar rapid lake growth was not followed by GLOFs in four other cases, casting doubts on the extensive use of this factor in GLOF susceptibility and hazard assessments (see the overview of [Kouglkoulos et al., 2018](#)).

### 5.4. Future lake evolution and triggering potential of GLOFs

There is a significant difference in glacier area remaining by the end of the 21st century under RCP 8.5 (24 km<sup>2</sup>) compared to RCP 2.6 (310 km<sup>2</sup>) (after [Schauwecker et al., 2017](#)). However, there is almost no difference in future lake development, and thereby GLOF triggering potential, under the two scenarios, with further expansion of glacial lakes in the Cordillera Blanca being limited because the glaciers that currently remain are typically steep and the underlying topography is therefore not suited for further lake expansion ([Fig. 6](#)). Already by 1948, 71% of the total area favorable for lake development in the region was occupied by lakes, increasing to 90% by 2018. A further expansion in overall lake area of around 10% therefore remains possible by the end of the 21st century, as depressions in the glacier bed topography are uncovered by retreating glaciers allowing existing lakes to expand and new lakes to emerge. Under RCP 8.5, lake development will have reached its maximum extent of 37 km<sup>2</sup> (considering only lakes >0.01 km<sup>2</sup>) by the end of the 21st century, while a further increase in overall lake area of just 2% (0.68 km<sup>2</sup>) remains possible under RCP 2.6. In total, 38 new lakes are expected to appear by the end of the 21st century under RCP 2.6, and 50 new lakes under RCP 8.5. The mean slope of the current surface topography beneath which these depressions are expected to form is 6.4° (STDEV 4.0°), confirming that the presence of flat glacial topography ([Section 4](#)) indeed provides a good first-order approximation of where future lakes are likely to develop.

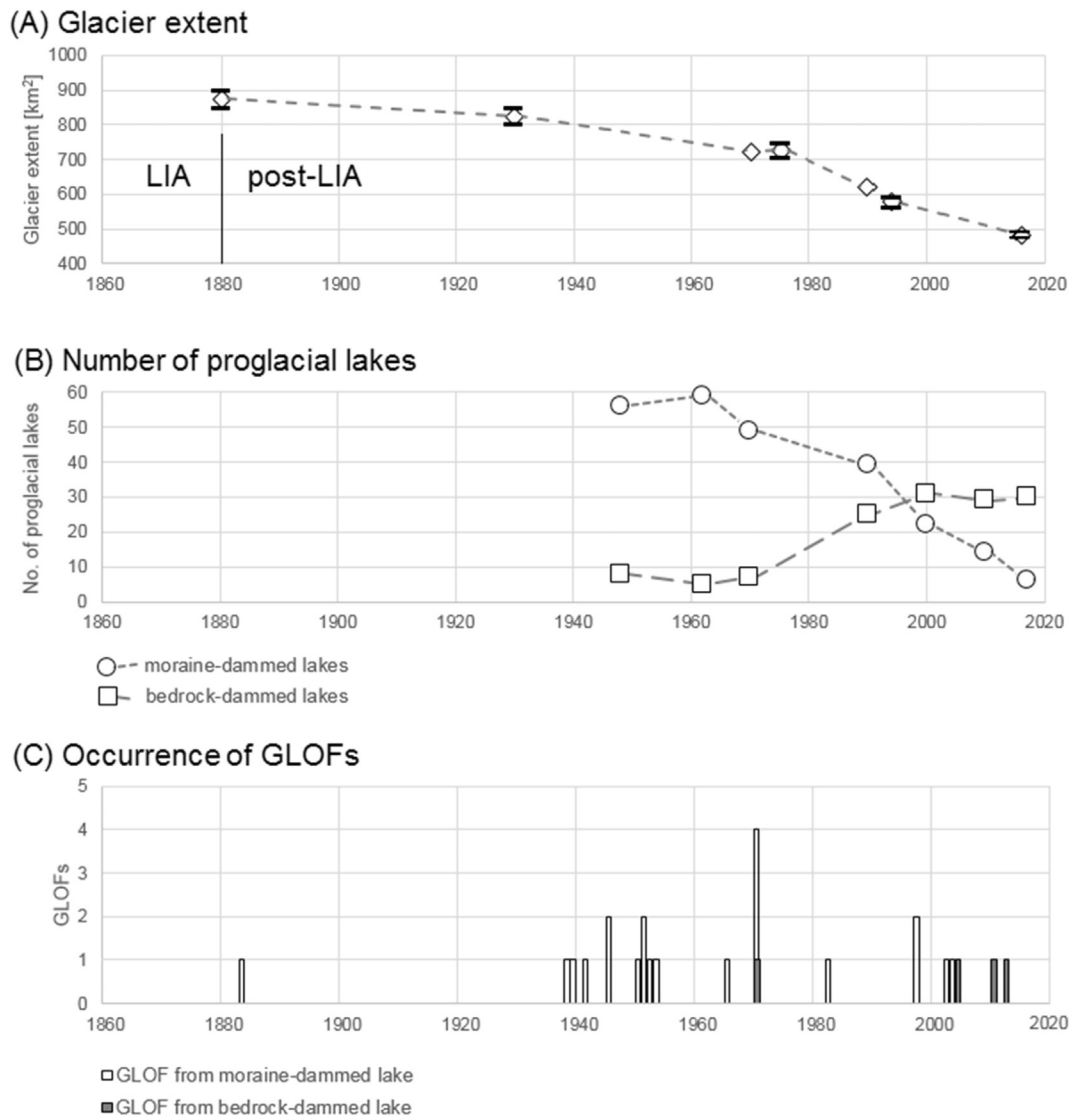


**Fig. 7.** The relationship between glacier extent (A), number of proglacial moraine- and bedrock-dammed lakes (B), and the occurrence of GLOFs from moraine-dammed and bedrock-dammed lakes (C).

More numerous lakes and a larger overall lake area increases the likelihood that mass movements of ice and/or rock can reach a lake and trigger an outburst event (Fig. 6). The increase in this triggering potential is almost linear with the increase in lake area ( $R^2 = 0.99$ ). Hence, there is no evidence that new and expanding lakes at higher elevation are individually more susceptible to impacts of rock and/or ice than those lakes that have already formed over the past century.

## 6. Discussion

### 6.1. GLOFs from bedrock-dammed lakes and possible secondary peak of GLOF occurrence

The conceptual model of Clague and Evans (2000) and the study of Harrison et al. (2018) only consider GLOFs originating from moraine-dammed lakes; it is, however, observed, that recent (post-2000) GLOFs in the Cordillera Blanca have originated predominantly from bedrock-dammed lakes (see Fig. S2). Moreover, the formation and evolution of bedrock-dammed lakes at higher elevation is observed and will continue to a limited extent in the future given ongoing glacier recession, considering the topographic setting of the region (Fig. 5), and the exposure of topographic overdeepenings at the glacial bed (Fig. 6)

(see also Cook et al., 2016; Emmer, 2017). In other words, we infer that observed glacier recession further upstream of the LIA moraines will change the focus from moraine- to bedrock-dammed lakes; a trend which is already being observed in lake inventories (see Fig. 4, Fig. 7A, B), a GLOFs inventory of the Cordillera Blanca (see Fig. 7C; Fig. S2) and in a record of newly formed lakes (see Fig. S1). From the perspective of the lag time concept, GRTs are comparable for both lake types (see Fig. S3). Bedrock-dammed lakes, however, have longer LRTs, it is therefore possible that a next GLOF peak frequency period, reflecting GLOFs from bedrock-dammed lakes, will appear in the near future. The exact shape, magnitude and timing (lag time) of this next peak is, however, as yet unclear.

The risk of a GLOF also increases as lakes increase their size, even if the number of GLOF triggers (e.g. rock falls) does not increase. This is because larger lakes represent a larger target than smaller lakes for landslides. Larger lakes also contain a larger amount of water available for potential flooding. This tendency is, however, counteracted by the increased resilience of large lakes to rock fall or moraine collapses. Therefore, assessing the GLOF risk must take into account increasing lake size as well as changes in trigger frequency, magnitude and type. In the Cordillera Blanca, the increase in potential GLOF triggering is demonstrated to increase linearly with increasing lake area. The situation is likely



different in other mountain regions where lakes remain primarily associated with large proglacial tongues and where significant potential therefore exists for these lakes to expand, and for new lakes to develop at higher elevation closer to steep mountain headwalls, increasing the triggering potential (see [Allen et al., 2016](#)). In the Cordillera Blanca, lake development is already at an advanced stage, and the potential for further expansion is rather limited.

### 6.2. Attribution of GLOF occurrence to climate forcing

Detection and attribution of observed extreme natural hazard events in high mountains to (anthropogenic) climate change is yet in its infancy but an important field to better understand the impact of climate change on these environments and downstream populations. It is used to distinguish between forced variability and unforced variability in a system; i.e. between systems whose behaviour is being driven by anthropogenic forcing of the climate, compared with behaviour of that system when driven only by natural variability of the climate. To develop detection and attribution for GLOFs, we would therefore need to have the data showing a clear and substantial record of GLOFs before the time when greenhouse gas (GHG) forcing had an important effect on the climate. Such a data would allow the comparison with a record of GLOFs under a GHG-driven climate.

At present, however, we do not have such a record and we speculate that GLOF frequencies peaked in the 1940s and 1950s and in the mid-late 1990s partly caused by enhanced glacier recession and increased precipitation during the major El Niño events in 1940–41 and 1997–98, which are widely reported in the literature. For instance, [Quinn et al. \(1987\)](#) use a range of qualitative and quantitative metrics including data from the Scientific Committee on Oceanic Research (SCOR) Working Group 55 to assess the strength of historical El Niño events. They identified the 1940–41 El Niño as a strong event, exceeded only by the 1982–83 event (and later also exceeded by the 1997–98 event). The strong 1997–98 El Niño began in Spring 1997 and by the summer was already the strongest El Niño since the beginning of instrumental observations with an Ocean El Niño Index above 2.00. This El Niño event brought flooding and mudslides across Peru and during December 1997–May 1998 Tumbes in northwestern Peru received ten times the precipitation recorded on average during this period. This exceptional amount of precipitation might be also responsible for three GLOFs which occurred in the Cordillera Blanca during the 1997–1998 El Niño event. A proper GLOF attribution analysis thus would need to distinguish between the effects of long-term climate and glacier change and short-term (extreme) events such as El Niño.

### 6.3. GLOF magnitude and potential impact of mitigation measures

Many of the GLOFs from moraine-dammed lakes in the Cordillera Blanca which occurred in the GLOF peak frequency period from 1938 to 1953 are characterized by their extreme magnitude (reach, volumes involved) compared to GLOFs which occurred later (see Fig. S2). In total, six extreme events are documented ([Emmer, 2017](#)), all of them during the peak frequency period in the first half of the 20th century or before (in 1725 and in 1883). This change is explained as a consequence of the shift from dam failures to smaller and lower volume dam overtoppings observed since the 1960s. Another reason might be the implementation of various types of mitigation measures (including lake remediation) since the 1940s ([Carey, 2005](#); [Emmer et al., 2018](#)). However, we do not expect these measures to completely prevent the occurrence of high-magnitude GLOFs, therefore, such events would still be visible in the record. Six documented GLOFs occurred from remediated lakes (in 1950, 1953, 1970, 2002, 2003, 2010) of which two GLOFs occurred during the peak frequency periods and three GLOFs during times of lake remediation, or as a result of failure of mitigation works. Overall, this leads to the conclusion that the peak frequency of GLOFs from moraine-

dammed lakes in the 1940s and 1950s is actually not being biased by the remediation efforts in the region.

The magnitude of GLOFs from bedrock-dammed lakes is expected to be generally lower compared to GLOFs induced by moraine dam failures, due to the smaller volumes involved (dam overtopping and lack of dam incision). Even smaller GLOFs from bedrock-dammed lakes upstream may, however, lead to process chains affecting large areas, especially in those cases where lakes downstream are involved ([Mergili et al., 2018](#); [Mergili et al., 2020](#)).

## 7. Conclusions

Our study demonstrates that the overall number of lakes as well as the total lake area in the Cordillera Blanca increased during the period 1948–2017, primarily driven by climate change-induced glacier retreat over the topographically suitable (overdeepened) terrain. We present the first region-wide evidence of the shift from moraine- to bedrock-dammed lakes among the newly formed lakes as well as among the GLOF-producing lakes. While this general pattern may be transferable to other mountain regions, the timing of this shift and implications for GLOF hazard will vary significantly depending on regional variations in lake development. Lake development is at an advanced stage in the Cordillera Blanca, with a further expected expansion in overall lake area of around 10% possible by the end of the 21st century. There is little difference in future lake development and GLOF triggering potential under the scenarios of RCP 2.6 and 8.5.

Detailed insight into the causes of GLOFs reveals a high share of triggers barely attributable to changing climate (e.g. earthquakes, landslides). Utilising these findings to explore the [Harrison et al. \(2018\)](#) model of GLOF occurrence, we conclude that climate change and topographical setting rather control the timing of GLOF-susceptible preconditions on a regional scale (i.e. the occurrence of proglacial lakes), while the GLOF occurrence is largely controlled by local factors and triggers, although some of these triggers such as calving processes might be associated with weather and climate conditions, highlighting the need for complex and multi-scale monitoring and assessment.

### Author contributions

AE initiated and drafted the outline of the study, analysed the evolution of lakes and past GLOFs. CH and HF supervised the work during the stay of AE at the University of Zurich. SH analysed climatological data, MM analysed topographical data and SA calculated the topographic potential for landslides and future lakes. All authors discussed and developed general conceptual approach and contributed to the process of writing and approved the final version of the manuscript.

### Declaration of competing interests

The authors declare that they have no known competing financial interests or personal relationships that could have appeared to influence the work reported in this paper.

### Data availability

Data are available on request from the corresponding author.

### Acknowledgment

This work was supported by The Ministry of Education, Youth and Sports of the Czech Republic within the National Sustainability Programme I (NPU I), grant number LO1415, and Supporting Perspective Human Resources Programme of the Czech Academy of Sciences, project “Dynamics and spatiotemporal patterns of glacial lakes evolution and their implications for risk management and adaptation in recently deglaciated areas” awarded to AE. CH was supported by the Glaciares+

project funded by the Swiss Agency for Development and Cooperation (SDC), and the Swiss National Science Foundation through the Project AguaFuturo (project no. 205121L.166272). Part of this work was supported by the RCUK-CONICYT project GLOP.

## Appendix A. Supplementary data

Supplementary data to this article can be found online at <https://doi.org/10.1016/j.geomorph.2020.107178>.

## References

- Ahmed, M., Anchukaitis, K.J., Asrat, A., Borgaonkar, H.P., Braid, M., Buckley, B.M., Büntgen, U., Chase, B.M., Christie, D.A., Cook, E.R., Curran, M.A.J., Diaz, H.F., Esper, J.E., Fan, Z.-X., Gaire, N.P., Ge, Q., Gergis, J., González-Rouco, J.F., Gooze, H., Grab, S.W., Graham, N., Graham, R., Grosjean, M., Hanhijärvi, S.T., Kaufman, D.S., Kiefer, T., Kimura, K., Korhola, A.A., Krusic, P.J., Lara, A., Lézine, A.-M., Ljungqvist, F.C., Lorrey, A.M., Luterbacher, J., Masson-Delmotte, V., McCarroll, D., McConnell, J.R., McKay, N.P., Morales, M.S., Moy, A.D., Mulvaney, R., Mundo, I.A., Nakatsuka, T., Nash, D.J., Neukom, R., Nicholson, S.E., Oerter, H., Palmer, J.G., Phipps, S.J., Prieto, M.R., Rivera, A., Sano, M., Severi, M., Shanahan, T.M., Shao, X., Shi, F., Sigl, M., Smerdon, J.E., Solomina, O.N., Steig, E.J., Stenni, B., Thamban, M., Trouet, V., Turney, C.S.M., Umer, M., van Ommen, T., Verschuren, D., Viau, A.E., Villalba, R., Vinther, B.M., von Gunten, L., Wagner, S., Wahl, E.R., Wanner, H., Werner, J.P., White, J.W.C., Yasue, K., Zorita, E., 2013. Continental-scale temperature variability during the past two millennia. *Nat. Geosci.* 6 (5), 339–346. <https://doi.org/10.1038/NGEO1797>.
- Allen, S.K., Cox, S.C., Owens, I.F., 2011. Rock avalanches and other landslides in the central southern alps of New Zealand: a regional study considering possible climate change impacts. *Landslides* 8 (1), 33–48. <https://doi.org/10.1007/s10346-010-0222-z>.
- Allen, S.K., Linsbauer, A., Randhawa, S.S., Huggel, C., Rana, P., Kumari, A., 2016. Glacial lake outburst flood risk in Himachal Pradesh, India: an integrative and anticipatory approach considering current and future threats. *Nat. Hazards* 84 (3), 1741–1763. <https://doi.org/10.1007/s11069-016-2511-x>.
- Allen, S.K., Zhang, G., Wang, W., Yao, T., Bolch, T., 2019. Potentially dangerous glacial lakes across the Tibetan Plateau revealed using a large-scale automated assessment approach. *Sci. Bull.* 64 (7), 435–445. <https://doi.org/10.1016/j.scib.2019.03.011>.
- Aziz, J.J., Ling, M., Rifal, H.S., Newell, C.J., Gonzales, J.R., 2003. MAROS: a decision support system for optimizing monitoring plans. *Ground Water* 41, 355–367. <https://doi.org/10.1111/j.1745-6584.2003.tb02605.x>.
- Bourrel, L., Rau, P., Dewitte, B., Labat, D., Lavado, W., Coutaud, A., Vera, A., Alvarado, A., Ordoñez, J., 2015. Low-frequency modulation and trend of the relationship between ENSO and precipitation along the northern to centre Peruvian Pacific coast. *Hydrol. Process.* 29 (6), 1252–1266. <https://doi.org/10.1002/hyp.10247>.
- Carey, M., 2005. Living and dying with glaciers: people's historical vulnerability to avalanches and outburst floods in Peru. *Glob. Planet. Chang.* 47 (2–4), 122–134. <https://doi.org/10.1016/j.gloplacha.2004.10.007>.
- Carey, M., Huggel, C., Bury, J., Portocarrero, C., Haeblerli, W., 2012. An integrated socio-environmental framework for glacier hazard management and climate change adaptation: lessons from Lake 513, Cordillera Blanca, Peru. *Clim. Chang.* 112 (3–4), 733–767. <https://doi.org/10.1007/s10584-011-0249-8>.
- Carrivick, J.L., Tweed, F.S., 2016. A global assessment of the societal impacts of glacier outburst floods. *Glob. Planet. Chang.* 144, 1–16. <https://doi.org/10.1016/j.gloplacha.2016.07.001>.
- Clague, J.J., Evans, S.G., 2000. A review of catastrophic drainage of moraine-dammed lakes in British Columbia. *Quat. Sci. Rev.* 19 (17–18), 1763–1783. [https://doi.org/10.1016/S0277-3791\(00\)00090-1](https://doi.org/10.1016/S0277-3791(00)00090-1).
- Clague, J.J., Huggel, C., Korup, O., McGuire, B., 2012. Climate change and hazardous processes in high mountains. *Rev. Asoc. Geol. Argent.* 69, 328–338.
- Coldwell, B., Clemens, J., Petford, N., 2011. Deep crustal melting in the Peruvian Andes: felsic magma generation during delamination and uplift. *Lithos* 125 (1–2), 272–286. <https://doi.org/10.1016/j.lithos.2011.02.011>.
- Colonia, D., Torres, J., Haeblerli, W., Schauerwecker, S., Braendle, E., Giraldez, C., Cochachin, A., 2017. Compiling an inventory of glacier-bed overdeepenings and potential new lakes in de-glaciating areas of the Peruvian Andes: approach, first results, and perspectives for adaptation to climate change. *Water* 9, 336. <https://doi.org/10.3390/w9050336>.
- Cook, J.S., Koukoulou, I., Edwards, L.A., Dortch, J., Hoffmann, D., 2016. Glacier change and glacial lake outburst flood risk in the Bolivian Andes. *Cryosphere* 10, 2399–2413. <https://doi.org/10.5194/tc-10-2399-2016>.
- Emmer, A., 2017. Geomorphologically effective floods from moraine-dammed lakes in the Cordillera Blanca, Peru. *Quat. Sci. Rev.* 177, 220–234. <https://doi.org/10.1016/j.quascirev.2017.10.028>.
- Emmer, A., 2018. GLOFs in the WOS: bibliometrics, geographies and global trends of research on glacial lake outburst floods (Web of Science, 1979–2016). *Nat. Hazards Earth Syst. Sci.* 18, 813–827. <https://doi.org/10.5194/nhess-18-813-2018>.
- Emmer, A., Klimeš, J., Mergili, M., Vilímek, V., Cochachin, A., 2016. 882 lakes of the Cordillera Blanca: an inventory, classification, evolution and assessment of susceptibility to outburst floods. *Catena* 147, 269–279. <https://doi.org/10.1016/j.catena.2016.07.032>.
- Emmer, A., Vilímek, V., Zapata, M.L., 2018. Hazard mitigation of glacial lake outburst floods in the Cordillera Blanca (Peru): the effectiveness of remedial works. *J. Flood Risk Manag.* 11 (S1), 489–501. <https://doi.org/10.1111/jfr3.12241>.
- Evans, S.G., Clague, J.J., 1994. Recent climatic change and catastrophic geomorphic processes in mountain environments. *Geomorphology* 10, 107–128. [https://doi.org/10.1016/0169-555X\(94\)90011-6](https://doi.org/10.1016/0169-555X(94)90011-6).
- Fischer, L., Purves, R.S., Huggel, C., Noetzi, J., Haeblerli, W., 2012. On the influence of topographic, geological and cryospheric factors on rock avalanches and rockfalls in high-mountain areas. *Nat. Hazards Earth Syst. Sci.* 12, 241–254. <https://doi.org/10.5194/nhess-12-241-2012>.
- Frey, H., Haeblerli, W., Linsbauer, A., Huggel, C., Paul, F., 2010. A multi-level strategy for anticipating future glacier lake formation and associated hazard potentials. *Nat. Hazards Earth Syst. Sci.* 10, 339–352. <https://doi.org/10.5194/nhess-10-339-2010>.
- Georges, C., 2004. 20th-century glacier fluctuations in the tropical Cordillera Blanca, Perú. *Arct. Antarct. Alp. Res.* 36 (1), 100–107. [https://doi.org/10.1657/1523-0430\(2004\)036\[0100:TGFTT\]2.0.CO;2](https://doi.org/10.1657/1523-0430(2004)036[0100:TGFTT]2.0.CO;2).
- Harrison, S., Kargel, J.S., Huggel, C., Reynolds, J., Shugar, D.H., Betts, R.A., Emmer, A., Glasser, N., Haritashya, U.K., Klimeš, J., Reinhardt, L., Schaub, Y., Willyshire, A., Regmi, D., Vilímek, V., 2018. Climate change and the global pattern of moraine-dammed glacial lake outburst floods. *Cryosphere* 12, 1195–1209. <https://doi.org/10.5194/tc-12-1195-2018>.
- Hidrandina, 1970. *Glacier Inventory of the Cordillera Blanca, 1962–70 shapefile*.
- Huss, M., Bookhagen, B., Huggel, C., Jacobsen, D., Bradley, R.S., Clague, J.J., Vuille, M., Buytaert, W., Cayan, D.R., Greenwood, G., Mark, B.G., Milner, A.M., Weingartner, R., Winder, M., 2017. Toward mountains without permanent snow and ice. *Earth's Future* 5 (5), 418–435. <https://doi.org/10.1002/2016EF000514>.
- IGM, 1975. *Mapa geológico del Perú 1:1.000.000*. Instituto de Geología y Minería (IGM), Lima, Peru.
- INAIGEM, 2016. *Glacier Inventory of the Cordillera Blanca 2016*. El Instituto Nacional de Investigación en Glaciares y Ecosistemas de Montaña (INAIGEM) shapefile.
- Iturrizaga, L., 2014. Glacial and glacially conditioned lake types in the Cordillera Blanca, Peru: a spatiotemporal conceptual approach. *Prog. Phys. Geogr.* 38 (5), 602–636. <https://doi.org/10.1177/0309133314546344>.
- Kaser, G., Osmaston, H., 2002. *Tropical Glaciers*. Cambridge University Press, Cambridge, UK.
- Klimeš, J., Novotný, J., Novotná, I., Jordán de Urries, B., Vilímek, V., Emmer, A., Strozzi, T., Kusák, M., Cochachin Rapre, A., Hartvich, F., Frey, H., 2016. Landslides in moraines as triggers of glacial lake outburst floods: example from Palcacocha Lake (Cordillera Blanca, Peru). *Landslides* 13 (6), 1461–1477. <https://doi.org/10.1007/s10346-016-0724-4>.
- Koukoulou, I., Cook, S.J., Jomelli, V., Clarke, L., Symeonakis, E., Dortch, J.M., Edwards, L.A., Merad, M., 2018. Use of multi-criteria decision analysis to identify potentially dangerous glacial lakes. *Sci. Total Environ.* 621, 1453–1466. <https://doi.org/10.1016/j.scitotenv.2017.10.083>.
- Linsbauer, A., Paul, F., Haeblerli, W., 2012. Modeling glacier thickness distribution and bed topography over entire mountain ranges with GlabTop: application of a fast and robust approach. *J. Geophys. Res.* 117, JF002313. <https://doi.org/10.1029/2011JF002313>.
- Llibouty, L., Morales, B.A., Pautre, A., Schneider, B., 1977. Glaciological problems set by the control of dangerous lakes in Cordillera Blanca, Peru. I. Historical failures of moranic dams, their causes and prevention. *J. Glaciol.* 18 (79), 239–254.
- Mann, M.E., Zhang, Z., Hughes, M.K., Bradley, R.S., Miller, S.K., Rutherford, S., 2008. Proxy-based reconstructions of hemispheric and global surface temperature variations over the past two millennia. *PNAS* 105, 13252–13257. <https://doi.org/10.1073/pnas.0805721105>.
- Maussion, F., Scherer, D., Mölg, T., Collier, E., Curio, J., Finkelnburg, R., 2014. Precipitation seasonality and variability over the Tibetan Plateau as resolved by the High Asia Reanalysis. *J. Clim.* 27 (5), 1910–1927. <https://doi.org/10.1175/JCLI-D-13-00282.1>.
- Mergili, M., Emmer, A., Juřicová, A., Cochachin, A., Fischer, J.-T., Huggel, C., Pudasaini, S.P., 2018. How well can we simulate complex hydro-geomorphic process chains? The 2012 multi-lake outburst flood in the Santa Cruz Valley (Cordillera Blanca, Perú). *Earth Surf. Process. Landf.* 43 (7), 1373–1389. <https://doi.org/10.1002/esp.4318>.
- Mergili, M., Pudasaini, S.P., Emmer, A., Fischer, J.-T., Cochachin, A., Frey, H., 2020. Reconstruction of the 1941 GLOF process chain at Lake Palcacocha (Cordillera Blanca, Perú). *Hydrol. Earth Syst. Sci.* 24, 93–114. <https://doi.org/10.5194/hess-24-93-2020>.
- Noetzi, J., Hoelzle, M., Haeblerli, W., 2003. Mountain permafrost and recent Alpine rock-fall events: a GIS-based approach to determine critical factors. In: Phillips, M., Springman, S.M., Arenson, L.U. (Eds.), *PERMAFROST Proceedings of the Eighth International Conference on Permafrost*. Swets & Zeitlinger, Zurich, Switzerland, pp. 827–832.
- Pánek, T., Korup, O., Lenart, J., Hradecký, J., Břežný, M., 2018. Giant landslides in the foreland of the Patagonian Ice Sheet. *Quat. Sci. Rev.* 194, 39–54. <https://doi.org/10.1016/j.quascirev.2018.06.028>.
- Paul, F., Linsbauer, A., 2012. Modeling of glacier bed topography from glacier outlines, central branch lines, and a DEM. *Int. J. Geogr. Inf. Sci.* 26, 1173–1190. <https://doi.org/10.1080/13658816.2011.627859>.
- Petrov, M.A., Sabitov, T.Y., Tomashevskaya, I.G., Glazirin, G.E., Chernomoret, S.S., Savernyuk, E.A., Tutubalina, O.V., Petrakov, D.A., Sokolov, L.S., Dokukin, M.D., Mountrakis, G., Ruiz-Villanueva, V., Stoffel, M., 2017. Glacial lake inventory and lake outburst potential in Uzbekistan. *Sci. Total Environ.* 592, 228–242. <https://doi.org/10.1016/j.scitotenv.2017.03.068>.
- Quinn, W.H., Neal, V.T., Antunez de Mayolo, S.E., 1987. *El Niño occurrences over the past four and a half centuries*. *J. Geophys. Res. Oceans Atmos.* 92 (C13), 14449–14461.
- Rabatel, A., Francou, B., Soruco, A., Gomez, J., Caceres, B., Ceballos, J.L., Basantes, R., Vuille, M., Sicart, J.E., Huggel, C., Scheel, M., Favier, V., Jomelli, V., Galarraga, R., Ginot, P., Maisincho, L., Mendoza, J., Menegoz, M., Ramirez, E., Ribstein, P., Suarez, V., Villacis, M., Wagnon, P., 2013. Current state of glaciers in the tropical Andes: a multi-century perspective on glacier evolution and climate change. *Cryosphere* 7 (1), 81–102. <https://doi.org/10.5194/tc-7-81-2013>.

- Rau, P., Bourrel, L., Labat, D., Melo, P., Dewitte, B., Frappart, F., Lavado, W., Felipe, O., 2017. Regionalization of rainfall over the Peruvian Pacific slope and coast. *Int. J. Climatol.* 37, 143–158. <https://doi.org/10.1002/joc.4693>.
- Rein, B., Lückge, A., Reinhardt, L., Sirocko, F., Wolf, A., Dullo, W.C., 2005. El Niño variability off Peru during the last 20,000 years. *Paleoceanography* 20 (4), PA4003. <https://doi.org/10.1029/2004PA001099>.
- Romstad, B., Harbitz, C., Domaas, U., 2009. A GIS method for assessment of rock slide tsunami hazard in all Norwegian lakes and reservoirs. *Nat. Hazards Earth Syst. Sci.* 9, 353–364. <https://doi.org/10.5194/nhess-9-353-2009>.
- Schaub, Y., 2015. *Outburst Floods from High-Mountain Lakes: Risk Analysis of Cascading Processes under Present and Future Conditions*. PhD thesis. Department of Geography, University of Zurich, Switzerland.
- Schauwecker, S., Rohrer, M., Acuna, D., Cochachin, A., Davila, L., Frey, H., Giraldez, C., Gomez, J., Huggel, C., Jacques-Coper, M., Loarte, E., Salzmann, N., Vuille, M., 2014. Climate trends and glacier retreat in the Cordillera Blanca, Peru, revisited. *Glob. Planet. Chang.* 119, 85–97. <https://doi.org/10.1016/j.gloplacha.2014.05.005>.
- Schauwecker, S., Rohrer, M., Huggel, C., Endries, J., Montoya, N., Neukom, R., Perry, B., Salzmann, N., Schwarb, M., Suarez, W., 2017. The freezing level in the tropical Andes, Peru: an indicator for present and future glacier extents. *J. Geophys. Res. Atmos.* 122 (10), 5172–5189. <https://doi.org/10.1002/2016JD025943>.
- Solomina, O., Jomelli, V., Kaser, G., Ames, A., Berger, B., Pouyaud, B., 2007. Lichenometry in the Cordillera Blanca, Peru: “Little Ice Age” moraine chronology. *Glob. Planet. Chang.* 59 (1–4), 225–235. <https://doi.org/10.1016/j.gloplacha.2006.11.016>.
- Sulca, J., Takahashi, K., Espinoza, J.C., Vuille, M., Lavado-Casimiro, W., 2018. Impacts of different ENSO flavors and tropical Pacific convection variability (ITCZ, SPCZ) on austral summer rainfall in South America, with a focus on Peru. *Int. J. Climatol.* 38 (1), 420–435. <https://doi.org/10.1002/joc.5185>.
- Thompson, L., Mosley-Thompson, E., Henderson, K., 2000. Ice-core paleoclimate records in tropical South America since the last glacial maximum. *J. Quat. Sci.* 15, 107–115.
- Veettil, B.K., 2018. Glacier mapping in the Cordillera Blanca, Peru, tropical Andes, using Sentinel-2 and Landsat data. *Singap. J. Trop. Geogr.* 39, 351–363. <https://doi.org/10.1111/sjtg.12247>.
- Veh, G., Korup, O., von Specht, S., Roessner, S., Walz, A., 2019. Unchanged frequency of moraine-dammed glacial lake outburst floods in the Himalaya. *Nat. Clim. Chang.* 9, 379–383. <https://doi.org/10.1038/s41558-019-0437-5>.
- Vilímek, V., Klimeš, J., Emmer, A., Novotný, J., 2014. Natural hazards in the Cordillera Blanca of Peru during the time of global climate change. In: Sassa, K. (Ed.), *Landslide Science for a Safer Geo-Environment*. Vol. 1. Springer, Switzerland, pp. 261–266.
- Vuille, M., Carey, M., Huggel, C., Buytaert, W., Rabatel, A., Jacobsen, D., Soruco, A., Villacis, M., Yarleque, C., Elison Timm, O., Condom, T., Salzmann, N., Sicart, J.-E., 2018. Rapid decline of snow and ice in the tropical Andes – impacts, uncertainties and challenges ahead. *Earth Sci. Rev.* 176, 195–213. <https://doi.org/10.1016/j.earscirev.2017.09.019>.
- Wilson, R., Glasser, N.F., Reynolds, J.M., Harrison, S., Iribarren Anaconda, P., Schaefer, M., Shannon, S., 2018. Glacial lakes of the Central and Patagonian Andes. *Glob. Planet. Chang.* 162, 275–291. <https://doi.org/10.1016/j.gloplacha.2018.01.004>.
- Zapata, M.L., 2002. La dinámica glaciar en lagunas de la Cordillera Blanca. *Acta Montana A.* 19 (123), 37–60.